Title
WAVE ENHANCED TRANSPORT IN AN ARC DISCHARGE

Authors
Wheeler, George M.
Pyle, Robert V.

Publication Date
1973-10-01

Submitted to Plasma Physics

LBL-2173
Preprint c.1

WAVE ENHANCED TRANSPORT IN AN ARC DISCHARGE

George M. Wheeler and Robert V. Pyle

October 1973

Prepared for the U. S. Atomic Energy Commission
under Contract W-7405-ENG-48

WAVE ENHANCED TRANSPORT IN AN ARC DISCHARGE*

George M. Wheeler† and Robert V. Pyle

Lawrence Berkeley Laboratory
University of California
Berkeley, California 94720, U. S. A.

October 1973

ABSTRACT

Enhanced particle transport due to a rotational flute instability in the plasma surrounding a hollow-cathode discharge was studied. The effect of enhanced transport on the plasma density profile was measured as a function of instability amplitude by changing potentials on end-ring boundaries. "End-ring stabilization" was observed to reduce enhanced transport by two orders of magnitude by reducing the radial electric field which drives the instability. The shape of the density profile could be explained by including enhanced transport in a simple diffusion theory for a cylindrical plasma with conducting boundaries.

1. INTRODUCTION

In many experiments in unstable or turbulent plasmas, anomalous particle transport is reported to be several orders of magnitude larger than predicted classically due to collisions. As a result, several theories have appeared in attempts to understand "wave-enhanced" transport. Different theories apply for different plasma conditions. For example, in a plasma exhibiting a broad band, incoherent-type turbulence, one would use a theory sensitive to the level, not necessarily the coherence, of the turbulent spectrum (BOHM et al., 1949; ICHIMARU and ROSENBLUTH, 1971). Often, however, coherent fluctuations are observed, peaked near one or more discrete frequencies; in this case, one might expect transport due to coherent oscillations to be important. The effect of coherent oscillations has been studied in quiescent plasmas(CHU et al., 1967; ELLIS and MOTLEY, 1971; MOTLEY and ELLIS, 1971), and in various discharges (SCHWIRZKE, 1964, 1966), including hollow-cathode discharges (YOSHIKAWA and ROSE, 1962; WARREN, 1968; HUDIS, 1969; NOON, et al., 1970; WHEELER and PYLE, 1973).

The present experiment was conducted in the weakly ionized plasma surrounding a hollow-cathode discharge in argon. The experimental conditions are discussed in Section 3. A rotational flute instability, driven largely by the radial electric field, has been discussed in an earlier paper (WHEELER and PYLE, 1973). The wave exhibited large-amplitude ($n_1/n_0 \lesssim 0.5$), coherent behavior. Wave-enhanced transport was determined from measurements of the density and potential fluctuations. CHU et al. (1967) studied enhanced plasma transport due to coherent drift waves in a Q-machine. They used an expression for net particle transport, F_{wave}, in terms of the correlation between the density and potential fluctuations: $F_{wave} = (n_1 \phi_1 / 2rB) \sin\psi$, where ψ is the phase between the density and potential fluctuations. Using this expression they inferred a wave "diffusion coefficient" (for purposes of numerical comparison only) an order of magnitude larger than collisional diffusion, and comparable in magnitude with Bohm diffusion. A density reduction of up to 30% in the central region and a density increase up to 6% at large radii were observed with the onset of instability.

NOON et al. (1970) used the above correlation expression to calculate a wave-induced ion current due to an ion-acoustic wave in a hollow-cathode discharge. The wave was reported as propagating obliquely to the discharge axis. However, the oscillation was weak, so that wave-enhanced transport was comparable in magnitude with collisional transport. Therefore, only small changes were observed on the density profile due to wave presence.

HUDIS (1969) was able to measure the cross-field particle transport velocity in a hollow-cathode discharge directly, using a rotating directional probe. He measured radial ion currents an order of magnitude larger than the Bohm value in the region of large centrifugal flute instability amplitude. The measurements of small changes in ion current (~ 0.1%) were quite difficult because radial currents were orders of magnitude smaller than currents along the magnetic field and drift currents. Fortunately, the measured radial current was in reasonable agreement with a calculated value, using the experimental wave amplitude. This result lends support to the reliability of the method of calculation of the transport rate.

In the present experiment, we estimated the magnitude of enhanced transport from the correlation between the density and potential fluctuations, which could be readily measured using Langmuir probes. In order to calculate the effect of transport on the density profile, we included enhanced transport in a simple diffusion theory for a cylindrical plasma with conducting axial boundaries. The resulting equation was then solved for the radial density profile, as a function of the transport coefficients. This theory is presented in Section 2 and compared with experimental findings in Section 4.

Various wave stabilization techniques, including feedback, were used to study radial plasma profiles as a function of instability amplitude and phase. One simple and effective technique involves the application of bias voltages to a configuration of five, concentric, conducting end-rings, which serve as the axial boundaries of the system. "End-ring stabilization" has the effect of eliminating or reducing the radial electric field at large radii, which we believe drives the rotational flute instability. Wave amplitude reduction is associated with steepening of the radial density profile. The effect is correlated with the results of the modified diffusion theory in Section 3.

2. PARTICLE TRANSPORT THEORY--SUMMARY

In the absence of local ionization and recombination, the radial plasma density profile is determined by the dominant transport mechanisms and the boundary conditions. The most important transverse transport mechanisms in our experiment were found to be weakly- and fully-ionized collisional diffusion, mobility in the radial electric field, and wave-enhanced transport (WARREN, 1968; WHEELER, 1972).

An expression for transport due to coherent low-frequency waves is obtained by considering the correlation between density and transverse velocity fluctuations. The net time-averaged transport can be written

$$\langle nv_r \rangle \equiv \frac{1}{2\tau} \int_{-\tau}^{\tau} n(t)v_r(t)dt. \qquad (1)$$

If we assume perturbations of the form exp $i(kr-\omega t)$, we obtain $\langle nv_r \rangle = (n_1 v_1/2)\cos\Delta$, where Δ is the phase by which the density fluctuation lags the velocity fluctuation. Unfortunately, the radial velocity fluctuation is rarely directly measurable. Often, however, in cylindrical geometry, the radial velocity fluctuation is largely due to a fluctuating azimuthal electric field, $v_{1r} \equiv E_\theta c/B = -ik\phi_1 c/B$. In this case, wave-enhanced transport has been expressed as (CHU et al., 1967)

$$\langle nv_r \rangle = \frac{n_1 \phi_1 c}{2rB} \sin\psi , \qquad (2)$$

where ψ is the phase by which the density fluctuation, n_1, leads the space potential fluctuation, ϕ_1.

The amplitude and phase of the density and floating potential fluctuations can be obtained from Langmuir probe data. The question then arises as to the relation between the space and floating potential fluctuations in the presence of electron temperature fluctuations. ELLIS and MOTLEY (1971) showed that the temperature fluctuations were important for determining the correct phase relationships for enhanced transport due to collisional drift waves in a Q-machine.

MOTLEY (1972) demonstrated that electron-emitting probes can be used to reduce the effect of temperature fluctuations on the space potential measurements. We have no experimental evidence on temperature fluctuations for the instability considered here. WARREN (1968) used gated probes to measure characteristics in a hollow-cathode discharge plasma at different times in the oscillation cycle of a higher frequency (48 kHz), different mode, and deduced apparent temperature changes of ±15%. Although measurements with either gated or emitting probes might give additional information, for the present we note that theory for the rotational flute instability shows that the phase between the density and space potential fluctuations is independent of electron temperature and consequently of temperature fluctuations [Eq. (5.27) of WHEELER, 1972; Eq. (10) of ILIĆ et al., 1973; and Eq. (11) of WHEELER and PYLE, 1973]. Electron temperature fluctuations are therefore neglected so that amplitude and phase of space potential fluctuations can be approximated by the directly measurable floating potential fluctuations. The effects of collisions and Coriolis force on phase were discussed elsewhere (WHEELER and PYLE, 1973).

In order to calculate the quantitative effect of enhanced transport on the shape of the density profile, a local "enhanced diffusion coefficient" is inferred:

$$D_{enh} \nabla n \equiv - \langle n v_r \rangle \, . \tag{3}$$

This expression is included in the particle transport equations in Appendix A. When ion mobility is neglected, a nearly exponential radial density variation is predicted, with density scale length,

$$q \doteq \frac{L}{\pi} \left[\frac{D_\perp}{D_{\parallel in}(1 + T_e/T_i)} \right]^{1/2} ,$$

where the effective transverse diffusion coefficient is defined as $D_{\perp} \equiv {}_{\perp in} + D_{\perp ei} + D_{enh}$, and L is the effective system length. Definitions for the classical transport coefficients are available in the literature (ALLIS, 1956; KAUFMAN, 1960; ROSE and CLARK, 1961).

Observations of the magnitude and parametric dependence of q often yield information on the magnitude and type of transport mechanisms present (YOSHIKAWA and ROSE, 1962; SCHWIRZKE, 1964, 1966; NOON et al., 1970). For example, if transport is predominantly classical in a strong magnetic field, B, then $q \sim B^{-1}$. If, however, enhanced transport of a type inversely proportional to B (e.g., Bohm diffusion) dominates, then $q \sim B^{-1/2}$. In the present experiment, the measured scale length is compared with a calculated value in an effort to determine the importance of wave-enhanced transport.

3. EXPERIMENTAL ARRANGEMENT

The present experiment was conducted in the weakly ionized plasma surrounding a hollow-cathode discharge, the properties of which are discussed in the literature (LIDSKY et al., 1962; HUDIS et al., 1968). The experimental arrangement is shown in Fig. 1. [The cathode assembly (anode A_I) was not used in the experiment.] An axial magnetic field, supplied by six modular coils, was varied from 580 to 1160 G. Cathode gas flow rates of 3 to 30 cm^3/min STP of argon were used, with a gas pressure of 3 to 10 mtorr in the cathode region and 0.2 to 3.0 mtorr in the diffusion chamber. Data is presented for discharge current I = 20 A. Cathode voltage with respect to the grounded anode and cylindrical walls was typically in the range -40 to -70 V.

At each end of the diffusion chamber (20-cm diameter, 58.2-cm long), the axial boundaries consisted of five concentric end-ring electrodes, mounted on an alumina insulating plate (Fig. 1b). The inner two rings were quartered to provide information on azimuthal symmetry, as well as to provide suitable suppressor electrodes for the application of linear feedback. All end-rings, the electrodes E_I, A_{II}, and E_{II}, and the diffusion region tank could be biased independently.

Langmuir probes were used as the primary diagnostic tool. All radial probes were inserted at the axial midplane. An axial probe could be rotated on its axis to provide axial plasma profiles at various radii and azimuths. A directional Langmuir probe, discussed by HUDIS and LIDSKY (1970), was employed in the present experiment to measure ion currents in the azimuthal and axial directions. We tested the accuracy and reliability of the directional probe by measuring directional currents in a microwave plasma device with a known streaming velocity (WHEELER, 1972).

4. RESULTS AND DISCUSSION

In the following experimental results, the electron temperature was obtained from a semilog plot of the probe I-V characteristic. The electron temperature decreased rapidly from ~ 3 eV near the central arc to less than 1 eV within 2 cm, and then decreased slowly to ~ 0.3 eV near the wall of the diffusion chamber. The ion temperature was calculated assuming heating by electrons and cooling by collisions with thermal neutral particles. The calculated ion temperature was in good agreement with the relation $T_i/T_e \cong 0.1$, which is used in the calculations (HUDIS et al., 1968).

The radial electric field strength was calculated using data from the directional Langmuir probe (HUDIS and LIDSKY, 1970). Azimuthal streaming currents were measured directly, from which the radial electric field was inferred. [The calculation of the electric field from azimuthal drift currents, including diamagnetic and centrifugal gravity drifts, is discussed in another paper (WHEELER and PYLE, 1973).] The electric field that was determined using this method, is reproducible to better than 10%, and is in agreement with the value obtained from the slope of the plasma potential, $\phi_p = \phi_f + \gamma(kT_e/e)$ with $\gamma = 1/2 \ln M_i/m_e = 5.6$ for argon.

We determined the effect of various potentials at the axial boundaries (Fig. 1b) on wave amplitude, and the effect of enhanced transport on the radial density profile. Of the various combinations of boundary potentials, we report two configurations. The radial and axial boundaries were grounded to anode potential in case (a), while the third end-rings (extending radially from 3.5 to 5.5 cm) were allowed to float electrically at +6 V in case (b). In both cases the axial magnetic field was B = 580 G, the discharge current was I = 20 A, and the pressure was p = 0.30 mtorr argon.

When the end-ring boundaries were grounded (at anode and wall potential), case (a), a large, nonuniform, nonambipolar, radial electric field appeared, shown in Fig. 2. In this case, a low-frequency (~ 2 kHz), m = - 1 (propagating in the ion-diamagnetic direction), flute instability was observed at large radii in the region of large, positive electric field. This instability has been "identified" as a rotational flute, driven by plasma rotation in the presence of a radial electric field (WHEELER and PYLE, 1973). The amplitude and phase profiles of the density and floating potential fluctuations have been recorded for various discharge and boundary conditions. From this data, expressions for wave-enhanced transport were calculated using Eq. (2).

The diffusion coefficients are shown in Fig. 3 for grounded end-rings, case (a). The expressions for the collisional diffusion coefficients and Bohm diffusion, calculated using experimental plasma parameters, are shown for comparison. We observe that D_{enh} at large radii is several orders of magnitude larger than classical, and is comparable in magnitude with Bohm diffusion. In Fig. 4 the density profile is observed to flatten out near the radius at which D_{enh} becomes larger than the collisional diffusion coefficients.

For case (b), when the third end-rings were allowed to float electrically, the radial electric field at large radii was greatly reduced or eliminated (Fig. 2). The resulting diffusion coefficients and density profile are shown in Figs. 3 and 4, respectively. With the primary destabilizing mechanism (E_r) reduced, we observe that D_{enh} is reduced by two orders of magnitude; and that the density profile is steeper, consistent with improved confinement. No significant change in electron temperature was observed.

(If one wanted to duplicate the conditions of case (b) using a power supply, 1.2 W must be supplied to the third end-ring to raise it to the floating potential of +6 V from ground potential, drawing a current of 0.20 A, ~ 1.8 mA/cm^2.)

When additional positive voltage (above the floating potential) was applied to the third end-ring, the wave was stabilized ($n_1/n_0 < 0.01$) with power levels required of about 1 W. The density profile was nearly exponential, as predicted by classical diffusion theory in the absence of fluctuations.

To show that the shape of the radial density profile could be explained by the effect of the wave, we included enhanced transport in a simple diffusion theory. The radial density scale length is calculated from Eq. (4) using experimental data and collision cross sections from the literature (GILBODY and HASTED, 1956). The calculated values are compared with the measured values, $q \equiv -(\nabla \ln n)^{-1}$, in Fig. 5 for both cases. The flattening of the profile, represented by the large scale length of Fig. 5a, can be explained by means of diffusion theory including enhanced transport.

5. CONCLUSION

The present work was directed primarily toward the study of wave-enhanced transport as a function of rotational flute instability amplitude. We used an expression for enhanced transport based on the correlation between the density and potential fluctuations. Using this expression we calculated an enhanced transport rate several orders of magnitude larger than the classical collisional rates, and comparable in magnitude with the Bohm rate.

Experimentally, we observed a flattening of the radial plasma density profile in the region of large wave amplitude. The flattening was largely attributed to wave-enhanced transport, which was the dominant mechanism.

The effect of wave-enhanced transport on plasma confinement was also investigated by adjusting potentials at the axial boundaries. By application of a bias voltage to a given end-ring configuration, we could vary the wave amplitude. For example, by merely floating the third end-ring electrically, the radial electric field, which drives the rotational flute instability, could be reduced with no external power requirements. The wave could be reduced or stabilized and the radial density profile would steepen, in agreement with our calculations, which include enhanced transport. Increased positive voltage consistently stabilized the wave (with power requirements ~ 1 W).

We conclude that concentric end-rings are effective in changing the radial electric field, and in stabilizing electric field-driven instabilities with small or no external power requirements. "End-ring stabilization" was observed to reduce enhanced transport by two orders of magnitude, causing ion density at large radii to decrease by one order of magnitude. In all cases, the shape of the radial density profile could be explained by including enhanced transport in a simple diffusion theory.

APPENDIX

Transport Theory

When a collisional plasma is confined under conditions such that a density gradient, an electric field, and coherent fluctuations exist, net particle currents are observed. The ion currents can be expressed as

$$nv_r = -(D_{\perp in} + D_{\perp ei})\frac{\partial n}{\partial r} + \mu_{\perp in} n E_r + \langle nv_r \rangle_{wave}$$

$$nv_z = -D_{\parallel in}\frac{\partial n}{\partial z} + \mu_{\parallel in} n E_z$$

where $D_{\alpha\beta}$ and $\mu_{\alpha\beta}$ are the standard diffusion and mobility coefficients for species α due to collisions with species β (ALLIS, 1956; KAUFMAN, 1960; ROSE and CLARK, 1961). These currents must be balanced by the particle conservation equation

$$\frac{\partial n}{\partial t} + \nabla \cdot (n\underline{v}) = - \alpha_R n^2 + \beta_I n ,$$

where recombination (α_R) and ionization (β_I) are estimated to be negligible in the secondary plasma of this hollow-cathode discharge (WARREN, 1968; WHEELER, 1972).

In order to solve these equations analytically for $n(r, z)$, we make the following assumptions:

(1) The electrons are in equilibrium along the magnetic field $n(z) = n_0 \exp(e\phi/kT_e)$ with the resulting axial electric field, $E_z = - (kT_e/e)[d(\ln n)/dz]$. This is a good assumption since most of the electrons are reflected at the end sheaths, and the Coulomb momentum-relaxation mean-free-path is much less than the system length.

(2) Cosinusoidal axial density dependence, $n(r, z) = n(r) \cos(\pi z/L)$, where L is the effective length of the diffusion region. This assumption is in good agreement with experiment.

(3) Enhanced transport can be expressed by means of an enhanced diffusion coefficient, $D_{enh} \nabla n \equiv - \langle n v_r \rangle$. This assumption has no physical basis, and merely allows us a convenient means to include enhanced transport quantitatively and analytically.

(4) Mobility in the radial electric field can be neglected. When a large radial electric field is present, mobility is important. In this case no analytic solution can be obtained for the ion density without specific assumptions about E_r. However, if E_r is small, as is often the case when stabilizing voltages are applied to the end-rings, then an analytic expression for the ion density profile can readily be obtained.

The relative importance of ion mobility can be estimated from the ratio of enhanced transport to ion mobility, $D_{enh}/(q\mu_{\perp in}E_r)$. The transverse ion mobility coefficient can be expressed in terms of the diffusion coefficient through the Einstein relation, $\mu_{\perp in} = eD_{\perp in}/kT_i$. Using data from the figures, we conclude that ion mobility around R = 5 cm is nearly an order of magnitude smaller than enhanced transport.

With assumptions (1) through (4), the ion continuity equation can be written

$$\frac{\partial n}{\partial t} = \frac{1}{r}\frac{\partial}{\partial r} rD_{\perp} \frac{\partial n}{\partial r} + \frac{\partial}{\partial z} D_{\parallel in}(1 + T_e/T_i)\frac{\partial n}{\partial z} = 0,$$

where the effective transverse diffusion coefficient is defined as $D_{\perp} \equiv D_{\perp in} + D_{\perp ei} + D_{enh}$. Using assumption (2), this reduces to Bessel's equation

$$\frac{1}{r}\frac{\partial}{\partial r} r\frac{\partial n(r)}{\partial r} - \frac{n(r)}{q^2} = 0,$$

where the density scale length is defined as

$$q = \frac{L}{\pi}\left[\frac{D_{\perp}}{D_{\parallel in}(1 + T_e/T_i)}\right]^{1/2} .$$

The solution to Bessel's equation can be written

$$n(r) = AK_0(r/q) + BI_0(r/q).$$

For q << r, which is reasonably valid in an hollow-cathode discharge for large radii, the Bessel functions of imaginary argument can be approximated

$$K_0(r/q) \approx \left(\frac{\pi q}{2r}\right)^{1/2} e^{-r/q},$$

$$I_0(r/q) \approx \left(\frac{q}{2\pi r}\right)^{1/2} e^{r/q} .$$

When $q << r$, a nearly exponential radial density variation is predicted, with radial scale length q.

FOOTNOTES

*This work was supported by the National Science Foundation and the U. S. Atomic Energy Commission.

†Present address: Institute for Plasma Research, Stanford University, Stanford, California 94305.

REFERENCES

ALLIS, W. P. (1956) Handbuch der Physik, Vol. XXI, p. 383, Springer-Verlag, Berlin.

BOHM, D., BURHOP, E. H. S. and MASSEY, H. S. W. (1949) The Use of Probes for Plasma Exploration in Strong Magnetic Fields, in The Characteristics of Electrical Discharges in Magnetic Fields, (Edited by A. Guthrie and R. K. Wakerling), Chapter 2. McGraw-Hill Book Co., New York.

CHU, T. K., HENDEL, H. W. and POLITZER, P. A. (1967) Phys. Rev. Lett. 19, 1110.

ELLIS, R. F. and MOTLEY, R. W. (1971) Proceedings of 3rd International Conference on Quiescent Plasmas, Elsinore, Denmark, p. 194.

GILBODY, H. B. and HASTED, J. B. (1956) Proc. Royal Soc. (London) A238, 334.

HUDIS, M., (1969) Particle Flux Measurements in a Hollow Cathode Arc, Ph. D. Thesis, Dept. of Nuclear Engineering, MIT.

HUDIS, M. and LIDSKY (1970) J. Appl. Phys. 41, 5011.

HUDIS, M., CHUNG, K. and ROSE, D. J. (1968) J. Appl. Phys. 39 3297.

ICHIMARU, S. and ROSENBLUTH, M. N. (1971) IAEA 4th Conference on Plasma Physics and Controlled Nuclear Fusion Research, Madison, Wisconsin, Paper CN-28/F2.

ILIĆ, D. B., ROGNLIEN, T. D., SELF, S. A. and CRAWFORD, F. W. (1973) Phys. Fluids 16, 1042.

KAUFMAN, A. N. (1960) in La Theorie des Gaz Neutres et Ionises (Edited by C. DeWitt and J. F. Detoeuf) p. 331. Wiley, New York.

LIDSKY, L. M., ROTHLEDER, S. D., ROSE, D. J., YOSHIKAWA, S., MICHELSON, C. and MACKLIN, R. J. Jr. (1962) J. Appl. Phys. 33, 2490.

MOTLEY, R. W. (1972) J. Appl. Phys. 43, 3711.

MOTLEY, R. W. and ELLIS, R. F. (1971) Phys. Fluids 14, 886.

NOON, J. H., SCHMIDT, H. A. and HOLT, E. H. (1970) Plasma Phys. 12, 477.

ROSE, D. J. and CLARK, M. Jr. (1961) Plasmas and Controlled Fusion p. 165. The MIT Press, Cambridge, Mass.

SCHWIRZKE, F. (1964) Phys. Fluids 7, 311.

SCHWIRZKE, F. (1966) Phys. Fluids 9, 2250.

WARREN, L. (1968) Transport of a Partially Ionized Plasma Across a Magnetic Field, Ph. D. Thesis, University of California, Berkeley. Lawrence Berkeley Laboratory Report UCRL-17601 (unpublished).

WHEELER, G. M. (1972) Low-Frequency Waves, Stabilization, and Enhanced Transport in the Plasma Surrounding a Hollow Cathode Discharge, Ph. D. Thesis, University of California, Berkeley, Lawrence Berkeley Laboratory Report LBL-577 (unpublished).

WHEELER, G. M. and PYLE, R. V. (1973) Phys. Fluids (to be published Dec. 1973).

YOSHIKAWA, S. and ROSE, D. J. (1962) Phys. Fluids 5, 334.

FIGURE LEGENDS

Fig. 1. The hollow-cathode discharge experiment is shown in (a). The concentric end-ring electrodes are shown in (b). Inner two tantalum end-rings are quartered; outer three rings are copper.

Fig. 2. Radial electric field for two end-ring voltage configurations: ●, all boundaries grounded, case (a), showing large positive E_r at large radii; ■, third end-rings are floated electrically, case (b), showing reduction of E_r. Lines are only to guide the eye.

Fig. 3. Diffusion coefficients. ●, D_{enh}(a) is the enhanced diffusion coefficient for the grounded case (a); ■, D_{enh}(b) showing reduced enhanced transport for the floating case (b). For comparison, ▼, D_{Bohm}; ◆, $D_{\perp ei}$, fully-ionized diffusion; and ▲, $D_{\perp in}$, ion-neutral diffusion are shown. Lines are only to guide the eye.

Fig. 4. Plasma density profiles for the grounded case (a), ●, and the floating case (b), ▲, showing flattening of the density profile in the presence of large wave amplitude. Lines are only to guide the eye.

Fig. 5. Radial density scale length, $q \equiv -(\nabla \ln n)^{-1}$. The upper curve is for the grounded case (a), showing flattening at large radii, while the lower curve is for the floating case (b). The scale length calculated from Eq. (4), is compared with the measured values, ●. Lines are only to guide the eye.

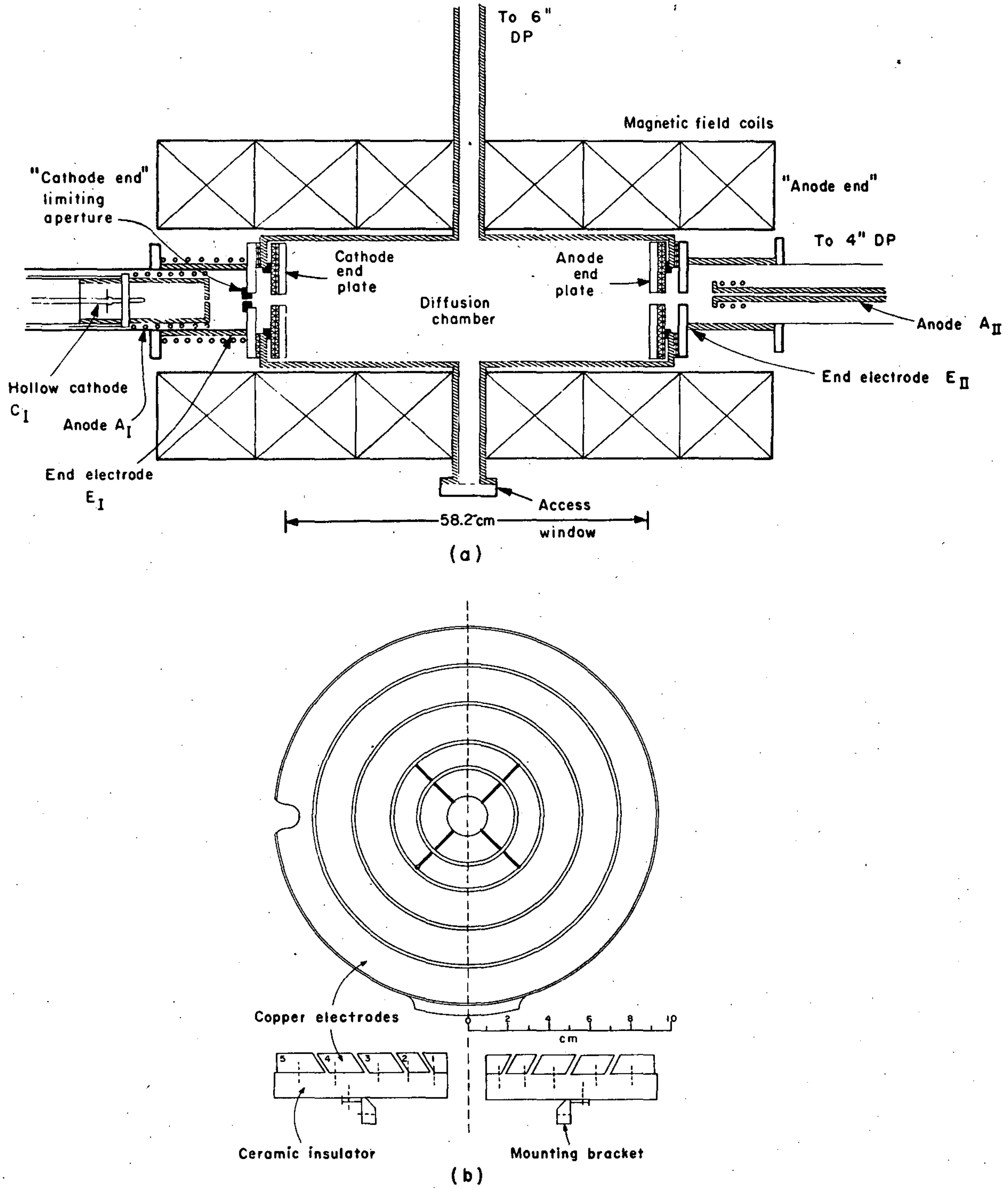

XBL739-4136

Fig. 1.

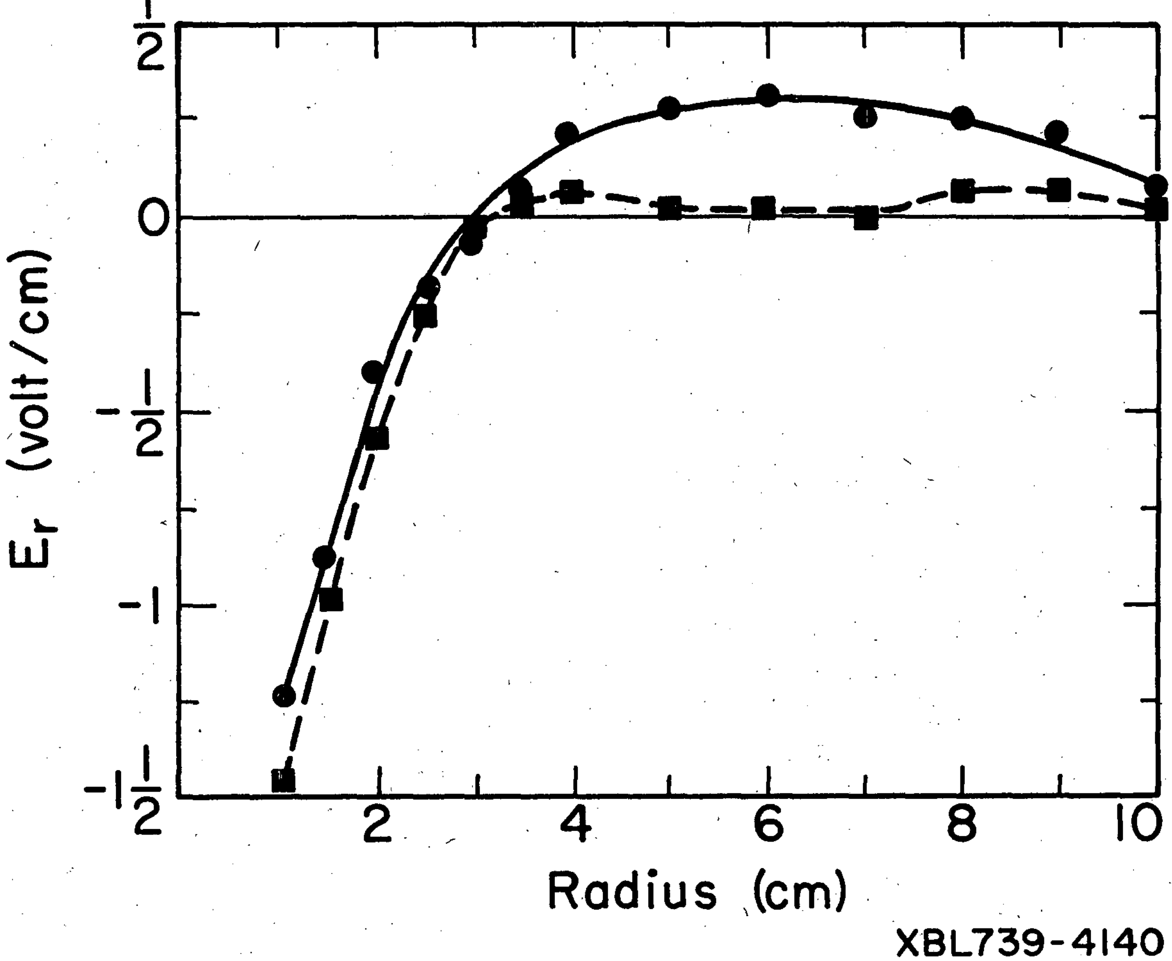

Fig. 2.

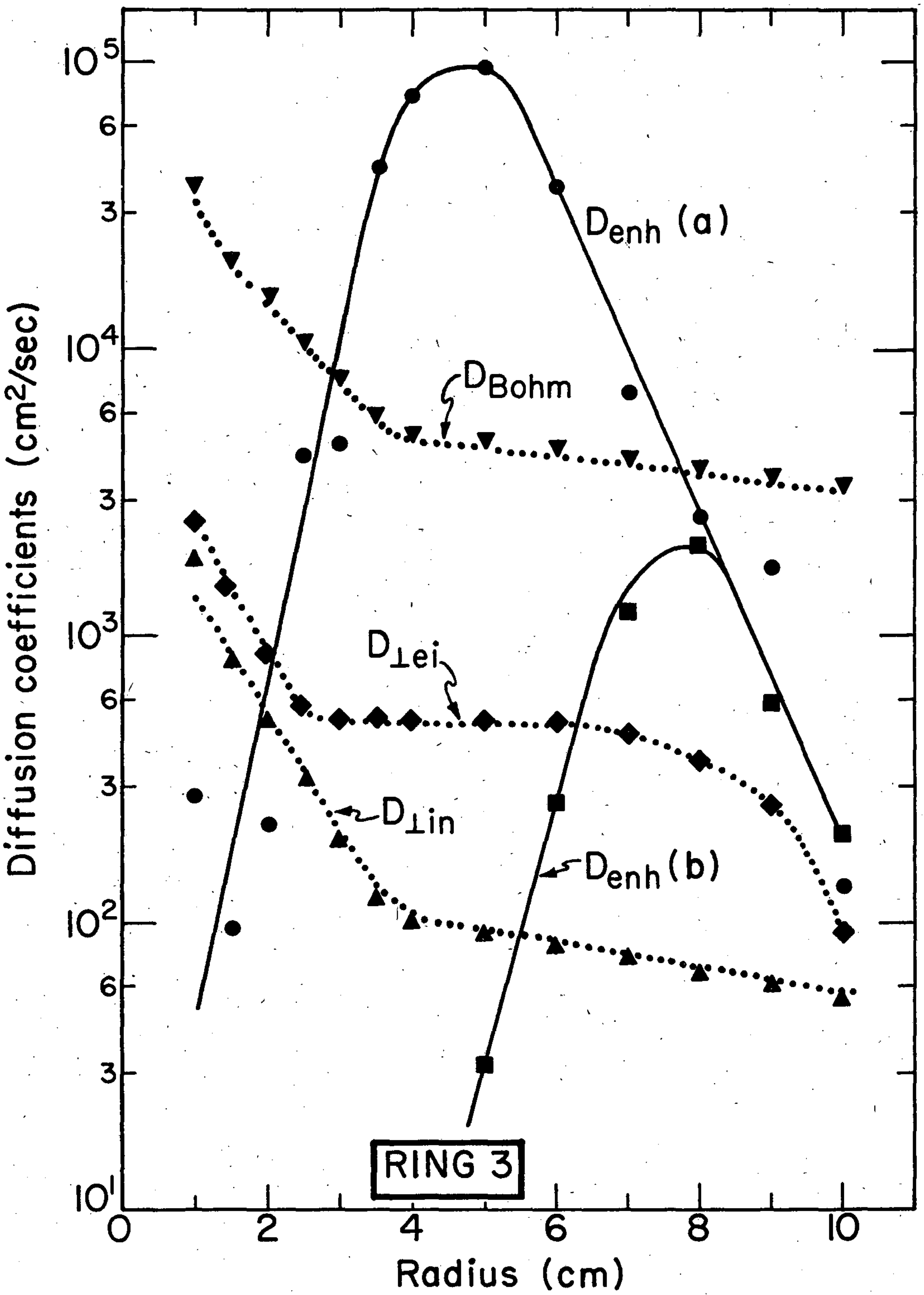

XBL739-4139

Fig. 3.

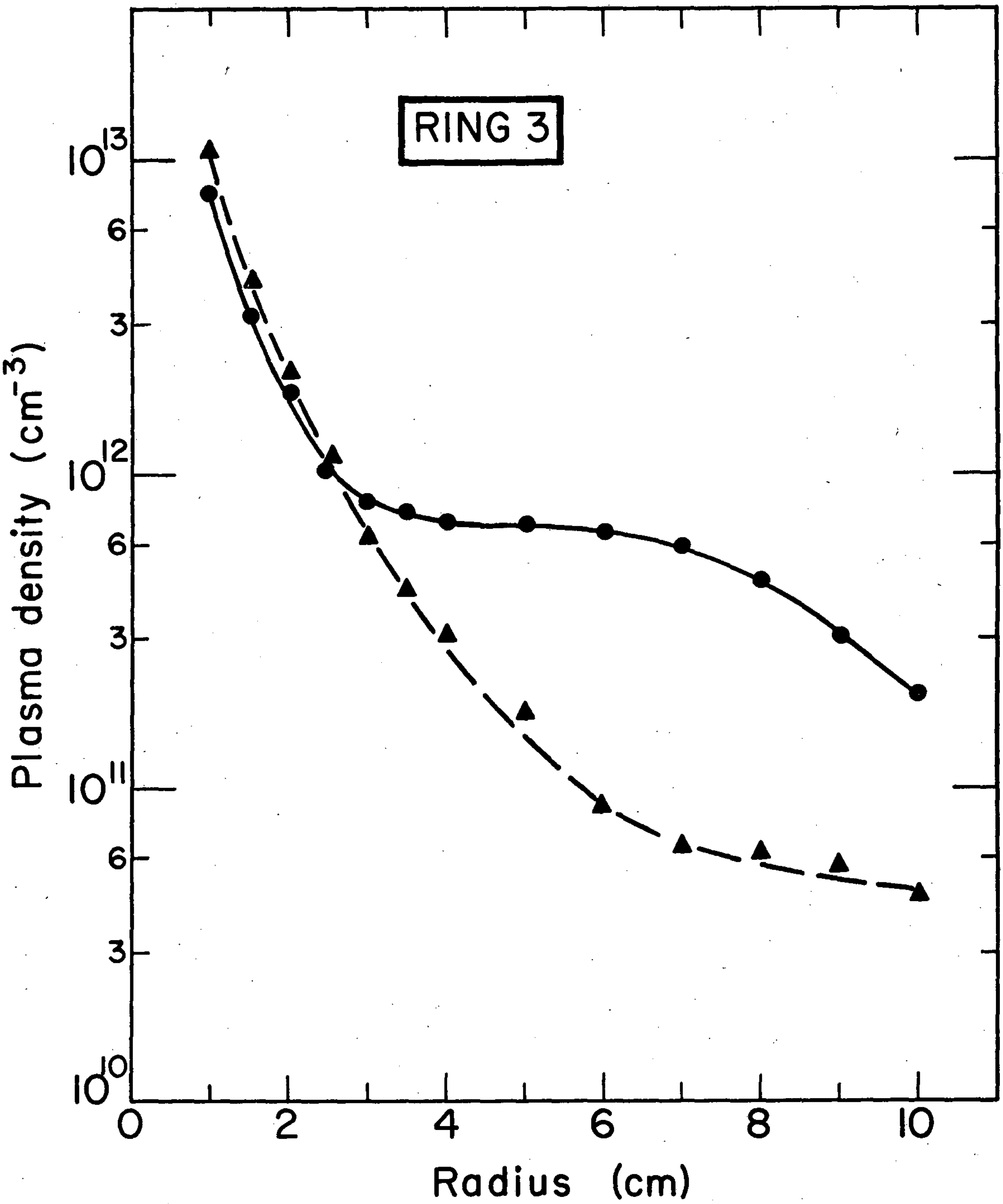

XBL739-4138

Fig. 4.

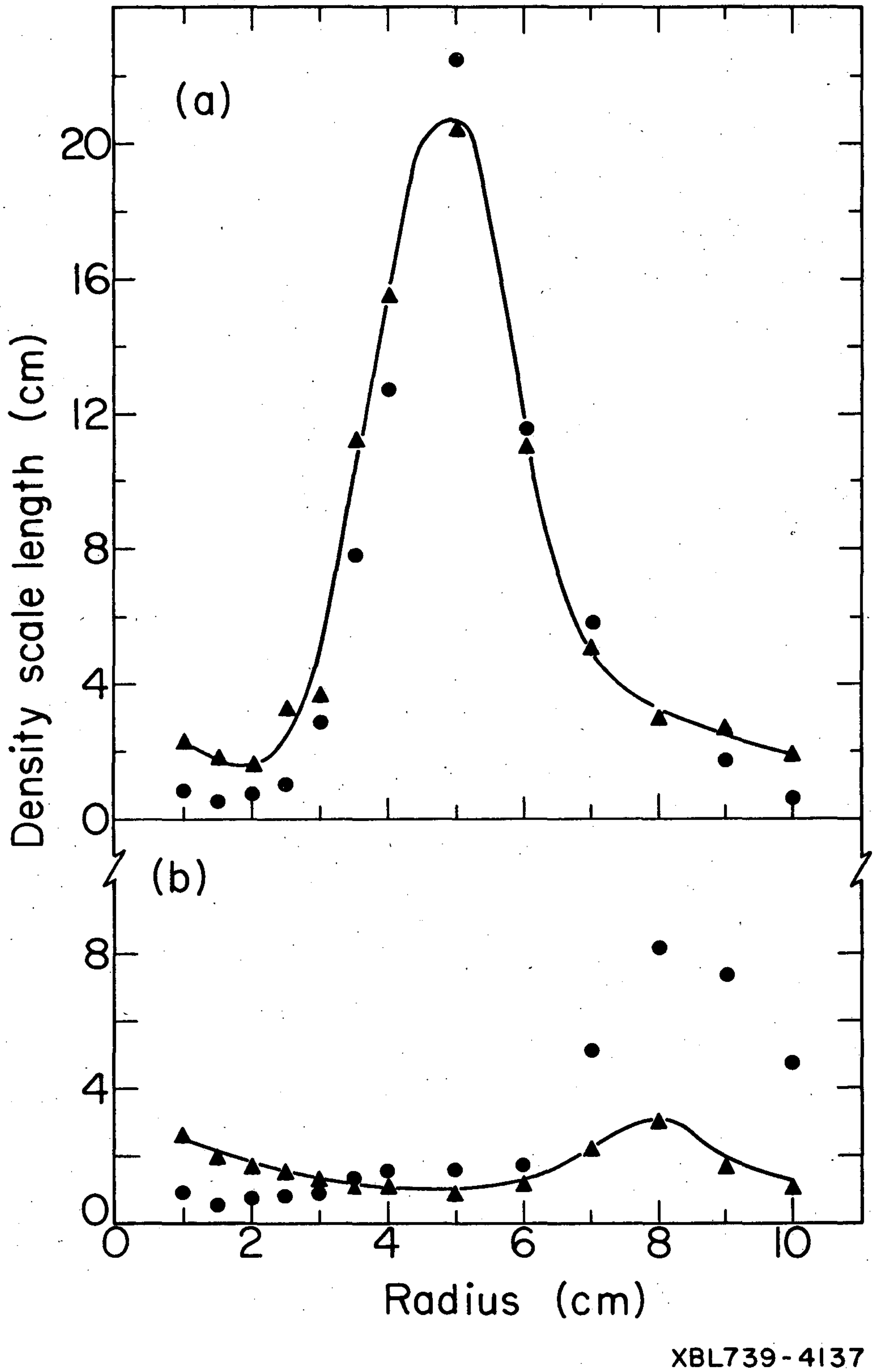
(a)
(b)
Density scale length (cm)
0
4
8
12
16
20
0
4
8
0
2
4
6
8
10
Radius (cm)
XBL739-4137

Fig. 5.

TECHNICAL INFORMATION DIVISION
LAWRENCE BERKELEY LABORATORY
UNIVERSITY OF CALIFORNIA
BERKELEY, CALIFORNIA 94720